Hindawi
Complexity
Volume 2022, Article ID 6322834, 15 pages
https://doi.org/10.1155/2022/6322834

Research Article

Fusion-Learning-Based Optimization: A Modified Metaheuristic Method for Lightweight High-Performance Concrete Design

Ghodrat Rahchamani,[1] **Seyed Mojtaba Movahedifar**,[1,2] **and Amin Honarbakhsh**[1,2]

[1]*Department of Civil Engineering, Neyshabur Branch, Islamic Azad University, Neyshabur, Iran*
[2]*New Materials Technology and Processing Research Center, Department of Civil Engineering, Neyshabur Branch, Islamic Azad University, Neyshabur, Iran*

Correspondence should be addressed to Amin Honarbakhsh; amin_honarbakhsh@yahoo.com

Received 1 June 2021; Revised 26 October 2021; Accepted 17 March 2022; Published 31 March 2022

Academic Editor: Haitham Afan

In order to build high-quality concrete, it is imperative to know the raw materials in advance. It is possible to accurately predict the quality of concrete and the amount of raw materials used using machine learning-enhanced methods. An automated process based on machine learning strategies is proposed in this paper for predicting the compressive strength of concrete. Fusion-learning-based optimization is used in the proposed approach to generate a strong learner by pooling support vector regression models. The SVR technique proposes an optimization method for finding the kernel radial basis function (RBF) parameters based on improving the innovative gunner algorithm (AIG). As a result of AIG's diverse solutions, local optima are effectively avoided. Therefore, the novelty of our research is that, in solving the uncertainty of predicted outputs based on integrated models, we use fusion-learning-based optimization to improve regression discrimination. We also collected a standard dataset to analyze the proposed algorithm, and subsequently, the dataset was designed from concrete laboratory tests on 244 samples, seven features, and three outputs. Different regression intensities are determined by correlation analysis of responses. Regression fusion is sufficiently accurate to estimate the number of desired outcomes examined based on the appropriate input data sample. The best quality concrete can be achieved with an error rate of less than 5%.

1. Introduction

The structural materials of concrete and the reaction between these materials play a critical and decisive role in explaining high-strength concrete's mechanical properties. Therefore, concrete designers and engineers seek to gain an accurate and thorough understanding of the relationship between the appropriate choice of type and amount of materials for concrete construction [1]. Concrete is a mixture of water, cement, and other materials, and from a chemical perspective, the strength of this material depends more than anything on cement and water [2]. High-strength concrete must exhibit resistance and flexibility against various forces and environmental factors. Hence, the proper mixture of raw materials can enhance the strength and quality of the concrete. The compressive strength of concrete depends on various factors, including mixing properties, mixing methods, mixing conditions, transport, and concrete [3]. Sometimes the concrete design engineer knows the initial composition and the estimated percentage of material mixing; however, the importance of an accurate estimate cannot be overestimated. Therefore, the concrete quality can only be assessed after making efficient concrete, and the elapse of a specific period, often a long interval (usually one month) using special tests [4]. Consequently, making quality concrete is conducted based on resembles a trial and error approach and may lead to extensive raw materials loss. By observing the falling slope in concrete, helpful information about the concrete performance can be obtained [5].

In addition, due to the great importance of concrete in structures and the significant growth of urbanization, the increase in demand for high-quality concrete is substantial

[6]. In many developing countries, such as China, the ready-mixed concrete, prepared by mixing concrete, dominates the entire concrete market [7]. As an advanced industry, the ready-mixed concrete trade is of utmost importance in significant sectors of industry and construction, transportation, and after-sales service. However, the current concrete industry management is still at the fundamental information management level because the knowledge generated during the management process is too complex to be used [8]. A goal-oriented and efficient way to address this problem is knowledge management and the adoption of artificial intelligence technology [9].

In recent decades, due to the proliferation of construction globally, a significant body of research has attempted to optimize the quality of concrete. Therefore, artificial intelligence (AI) has received growing attention as an analyzer of information in this field. The main application of soft computing-based methods is to determine concrete strength [10–18]. Most researchers focus on accurate estimation of raw materials based on artificial neural networks (ANNs) ability to estimate correct regression outputs [19–21]. Some researchers have also used ANN and clustering methods such as adaptive neuro-fuzzy inference system (ANFIS) [22]. In other studies, rapid learning and its combination with Cascade-forward neural network (CfNN) have been highlighted, which has led to the decreased processing time of concrete ingredients and achievement of the desired output [23]. Some investigations have utilized a combination of neural networks and evolutionary algorithms or metaheuristic (MH) to improve the precision of obtaining desired outcome [24, 25]. Combination with evolutionary algorithms (EA) is typically intended to amend inherent defects of ANN or other regression-based estimation methods. These algorithms are extensively used in ANN training for accurate error estimation. These include the genetic algorithm (GA) [26, 27], particle swarm optimization (PSO) [28], or simulated annealing (SA) [29]. The genetic algorithm can find global and local optimums and may be even trapped in local optimums, but it has rapid convergence [26, 27]. A growing number of studies have recently adopted ANN [27, 28, 30] and SVR [29] as a model for regression network estimation. The utilization of methods such as deep learning to estimate the quality of concrete has drawn considerable attention, urging researchers to adopt different deep learning models to improve the quality of concrete [31–33]. Sadrossadat and others. [34] have developed an evolutionary-based prediction model of the 28-day compressive strength of high-performance concrete containing cementitious materials.

Estimating the concrete performance is an essential process in ensuring the quality of various concrete components. Concrete testing is a method that measures near-performance parameters and provides valuable information about these parameters. The methods currently used in the world measure the stability of concrete in the laboratory or on-site. In some experiments, a kind of failure is estimated by measuring the reduction in the upper surface of freshly crushed concrete. Low accuracy, uncertainty, computational complexity, and the lack of a generalized method in the automatic determination of concrete raw materials in previous strategies have led us to look for more appropriate and accurate solutions.

Given that specific percentages of materials need to be combined to produce concrete of varying grades, this process is usually based on personal experience, and trial and error deems necessary to avoid wasting materials. For this to happen, an automated method is required for the analysis of raw materials. The importance of research becomes more apparent, knowing that a significant portion of its constituents include water, cement, and sand and are among finite resources that are rapidly depleted. Therefore, either one must possess exceptional skills and expertise, or a solution must be found to estimate the precise percentage of ingredients. Thus, the previous automated models are highly dependent on the optimized regression-learning model and the input components selection. Concrete design decisions on the component level must be correlated to operational cost and emissions on the supply chain level to evaluate commercial and environmental influence [35]. The main difficulty is finding a qualified approach to produce proper outputs on concrete designing in the real world. Fitting outputs are achieved by relying on appropriate learning methods. Recently, the relevant studies have considered optimization algorithms based on support vector models for high-quality concrete design [36–40].

Although both SVR and ANN models can map input data to a higher dimensional space to determine the decision boundary, NNs require numerous data input than SVR to better training. In addition, SVRs need minimal or more negligible processing of input data, which saves a lot of time. Besides, the ANN model usually necessitates much more modification, cleaning, data processing, etc. Typically the ANNs involve batch conversion to numbers, feature scaling, etc.

In the current study, we present an effective prediction design of concrete structure based on the proper fusion model of Support Vector Regression (SVR) learner and innovative gunner algorithm (AIG). Also, the AIG algorithm is described by a significant search space exploration, owing to solution vectors, typical for swarming techniques. Thus, the AIG algorithm achieves diverse solutions, which provides it high efficiency in avoiding local optima [41]. Besides, it can be utilized successfully to determine target functions of different shapes and with multiple optima and multidimensional functions.

The proposed method can remarkably reduce the classification error in regression mode to design lightweight and high-performance concrete. Our model has produced desirable results for predicting 28-day compressive strength and helps save the raw materials for concrete production. The method has been applied to a set of laboratory data collected by the authors. Similarly, attempts have been made for innovation to generate actual data in the laboratory within three months and fabricate different concrete types with varying qualities.

The remainder of this paper is organized as follows: the method components are described in Section 3. Section 4 introduces the proposed model, including the used

optimization algorithm and the regression learner. Section 5 presents the results and interpretations of the classification under various conditions. Finally, the paper is concluded by summarizing the key points in Section 6.

2. Contribution and Learning Structure

In this section, the components we utilized to optimize the concrete quality prediction based on learning process are described. As shown in Figure 1, the significant contributions of designing lightweight and high-performance concrete have been related to data development, automated analysis of outputs (i.e., effective design), and best learning to discriminate concrete quality.

2.1. Regression Learning. Assuming that one training data is available, if each input has D attributes (i.e., belongs to the D-dimensional space), and each point is assumed to have Y corresponding special, a function can be found that relates the input to the output [42]:

$$f(x, w) = w^T x + b. \tag{1}$$

To obtain the function f, the values of w and b in the following equation must be minimized:

$$R = \frac{1}{2}\|w\|^2 + C_1 \frac{1}{l} \sum_{i=1}^{l} L_\varepsilon (y_i, f_i(x, w)), \tag{2}$$

where C_1 is a constant value, the value of which is set by the user. The C_1 value is intended to create balance and change the weights of the penalty due to the omission of the variable ε and, at the same time, maximize the margin for discrimination. Accordingly, function L_ε is introduced according to

$$|y - f(x, w)|_\varepsilon = \begin{cases} 0, & |y - f(x, w)| \le \varepsilon, \\ |y - f(x, w)| - \varepsilon, & \text{otherwise.} \end{cases} \tag{3}$$

The equation is rewritten as a maximum of the following equation [43]:

$$L_P(a_i, a_i^*) = -\frac{1}{2} \sum_{j=1}^{l} (a_i - a_i^*)\left(a_j - a_j^*\right) x_i^T x_j - \varepsilon \sum_{i=1}^{l} (a_i + a_i^*) + \sum_{i=1}^{l} (a_i - a_i^*) y_i, \tag{4}$$

where conditions are defined based on

$$\text{Condition: } \begin{cases} \sum_{j=1}^{l} (a_i - a_i^*) = 0, \\ 0 \le a_i \le C, \quad i = 1, \ldots, l, \\ 0 \le a_i^* \le C, \quad i = 1, \ldots, l. \end{cases} \tag{5}$$

By solving the above equations, the SVR function, i.e., f in (1), can be obtained using the kernel function:

$$f(x, w) = w_0^T x + b = \sum_{j=1}^{l} (a_i - a_i^*) x_i^T x + b. \tag{6}$$

2.2. Innovative Gunner Algorithm (AIG). According to Newton's law, a projectile's motion can be directed vertically in a homogeneous gravitational field where the initial velocity in the horizontal direction is not zero [41]. A projectile is thrown with the initial velocity v_0 at an angle δ, and its horizontal surface is assumed to be perpendicular to the direction of gravity. It has a parabolic motion in a frame with dimensions d and h. This equation is defined according to (7), where g denotes the acceleration caused by the gravitational force:

$$h = \tan\,\delta.d - \frac{g.d^2}{2.v_0^2.\,\cos^2\,\delta}. \tag{7}$$

Computations will be more complicated if drag forces are involved. For the simplest model, where the tensile force is assumed to be proportional to the velocity of the projectile, (7) will be significantly complicated because [41]

$$h = \left(\tan\,\delta + \frac{g}{k.v_0.\,\cos\,\delta}\right).\mathrm{d} + \frac{g}{k^2}\,.\,\ln\left(1 - \frac{\mathrm{d}.k}{v_0.\,\cos\,\delta}\right), \tag{8}$$

where k is defined as drag coefficient (unit 1/s), and its value depends on weight and air resistance. Several analytical and experimental methods have been proposed to ensure the accuracy of the projectiles equations based on ballistics. Figure 2 shows the bullet motion curve for three different angles.

However, it should be noted that the actual projectile curve can be expressed as

$$h = \left(\tan\,\delta + \frac{g}{k.v_0.\,\cos\,\delta}\right).\mathrm{d} + \frac{g}{k^2}.\,\ln\left(1 - \frac{\mathrm{d}.k}{v_0.\,\cos\,\delta}\right) + f_h(\xi), \tag{9}$$

where $f_h(\xi)$ is a function influenced by interfering factors, including changes in air resistance, temperature, wind, shape, and motion of the Earth. In this case, the angle δ can be assumed as a decision variable for the optimization process, whose objective function is as follows:

$$F_{obj}(\delta) = |h(\delta)| \mapsto \min. \tag{10}$$

Given the complex form of equation (10) and the uncertainty of the function $f_h(\xi)$, a metaheuristic method could be used to calculate the value of angle and firing.

3. Proposed Method

Figure 3 shows the overall steps for the suggested implementation of concrete designing.

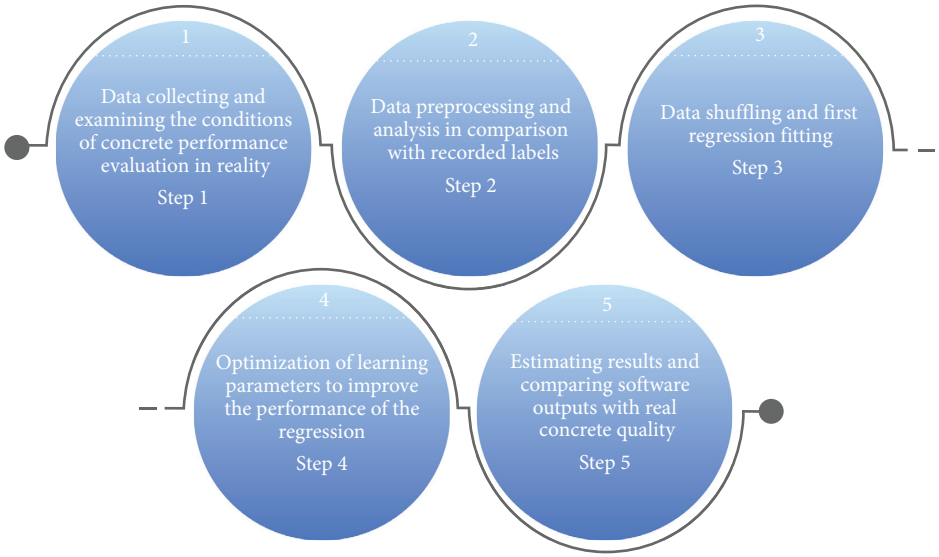

Figure 1: A general schematic of the main contributions in concrete quality prediction.

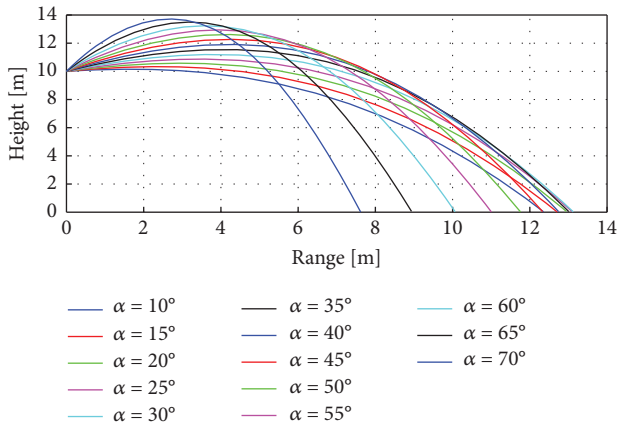

Figure 2: Bullet motion curve for three different angles.

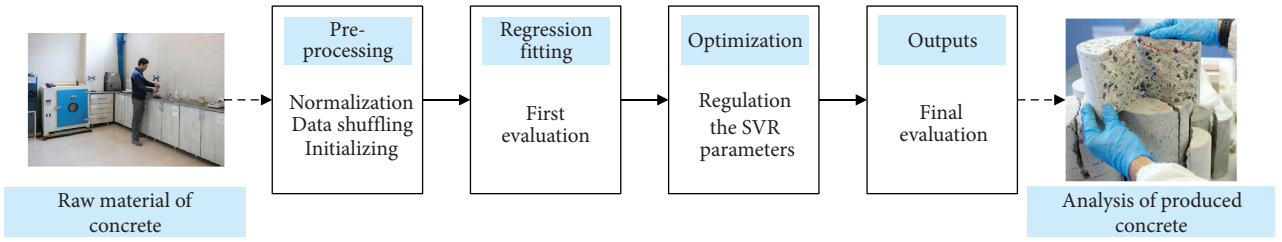

Figure 3: This diagram shows the overall design for the proposed implementation method.

3.1. Preprocessing. First, as shown in Figure 4, we shuffled the data in the preprocessing step to prevent overtraining of the automatic classification procedure. Although the samples are randomly mixed, the label's position changes regularly according to the classes of each received sample. We are applying such a method to prevent overfitting, leading to a considerable increase in classification accuracy. Because each data's concrete is intrinsically highly distributed and uses numerous diverse samples in a wide range, they must be normalized in the next step of the preprocessing step. Normalization of samples reduces the processing cost and positively affects the optimization of concrete quality prediction [44].

$$Y_{\text{norm}} = \frac{Y_s - Y_{s_{\min}}}{Y_{s_{\max}} - Y_{s_{\min}}}. \tag{11}$$

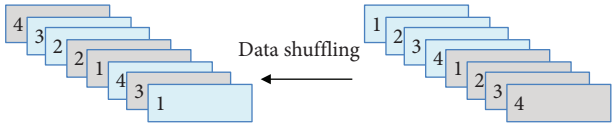

Figure 4: Data shuffling in preprocessing step.

Y_{norm} is considered the normalized value, and the variables Y_{smin} and $Y_{S_{max}}$ are the minimum and maximum values, respectively. Besides, Y_s is the current value of the concrete sample under study.

3.2. Fusion Regression. In the first step, data normalization is performed. This process is conducted using the Min-Max method to reduce excessive dispersion of data. The main goal of support vector machines is to find an optimal hyper-plane as a decision-making level that maximizes the margin between two classes. The data are moved to a considerably larger space by the Φ kernel function to classify highly complex data. The kernel function maps data from the input space on a space with higher dimensions, so that it is possible to separate the data in that space linearly. In the first part, the SVR regression learning pool as regression fusion model is used by applying training data. The general diagram is shown in Figure 5 and depicts the general learning framework. The initialization of γ and s for each regression classifier is initially randomized. The change interval for these two parameters varies from zero to 20. By applying the training data, the structure with the lowest mean square error (MSE) is selected, and its parameters *?* and *s* are given to input to the AIG algorithm. In this way, convergence towards the optimal response is faster and more accurate. The regression fusion of pool structure is evaluated by five repetitions, averaging accuracy, and finding the best corresponding parameters. The best matching parameter is a grid with the highest accuracy rate. In addition, finding the best RBF kernel values facilitates the search for the global optimum in the modified AIG algorithm.

3.3. Improving the Best Model. In order to optimize the model parameters, various methods can be used. The space networked with RBF kernel was identified as the best kernel for the data [45, 46]. This kernel can be expressed for two variables and *b*:

$$K(a,b) = \exp\left(-\gamma\|a-b\|^2\right) = \exp\left(-\frac{\|a-b\|^2}{2\sigma^2}\right), \quad (12)$$

where the parameter γ corresponds to the square of the width of Gaussian kernel. By finding the initial values γ and C in the classification pool, the modified AIG algorithm is used by accounting for air resistant. This constraint is considered more than other constraints for $f_h(\xi)$ because other constraints do not always exist in real conditions, but air resistance is present under almost any condition.

The most typical case of air resistance, for Reynolds numbers above 1000, is Newton drag with a drag force proportional to the speed squared, $F_{air} = -kv^2$. In air, which has a kinematic viscosity around 0.15 cm^2/s, this means that the product of speed and diameter must be greater than about 0.015 m^2/s. Unfortunately, the equations of motion cannot be easily solved analytically for this case. Therefore, a numerical solution will be examined.

$$F_D = -\frac{1}{2} c\,\rho\,A\,v\,V, \quad (13)$$

where F_D, c, ρ and A are defined as drag force, drag coefficient, air density, and cross sectional area of the projectile, respectively, and μ is defined according to

$$\mu = \frac{k}{m} = \frac{c\rho A}{(2m)}. \quad (14)$$

In light of these limitations and initialization in the previous step, the fitness function is defined in the metaheuristic algorithm, according to MSE. The termination condition of the algorithm is based on calculating the minimum error of MSE. Suppose that the algorithm is not realized in a certain number of iterations. In that case, the parameters matching the best regression network are selected, which produce a more significant effect on regression learning than other SVR structures do. On the other hand, considering the drag conditions and air resistance, the shot angle widens, and the best angle is set between 30 and 80°. According to the calculations, the best shot angle is 45°, but in changing the initial velocity of the bullet, the optimal angle is altered considering air resistance.

4. Experimental Results

The proposed method was implemented by MATLAB R2019b in Windows 10 operating system. The hardware platform used for simulation was an Intel® Core ™ i5-8500 system with 8 GB of RAM, plus 16 GB of SSD RAM. Other complementary software such as SPSS was also used. The input data were incorporated into an integrated algorithm, and the inputs were normalized in the first step. Mean square error (MSE) and mean absolute percentage error (MAPE) are expressed in (15) and (16), respectively. They were tested using adaptive algorithms in input analysis.

$$\text{MAPE} = \frac{1}{N}\sum_{i=1}^{N}\frac{|T_i - P_i|}{T_i}. \quad (15)$$

$$\text{MSE} = \frac{1}{N}\sum_{i=1}^{N}(T_i - P)^2. \quad (16)$$

In these equations, T_i, P_i, and N are the actual output values, the values predicted by the algorithm, and all specimens. In addition to the MSE and MAPE calculation, the maximum and minimum errors were also estimated, and the results of the K-fold cross-validation were calculated for each test.

4.1. Dataset. Data were obtained from the concrete testing laboratory at Imam Khomeini University of Sabzevar, Iran, over six months. The data consists of seven inputs and three

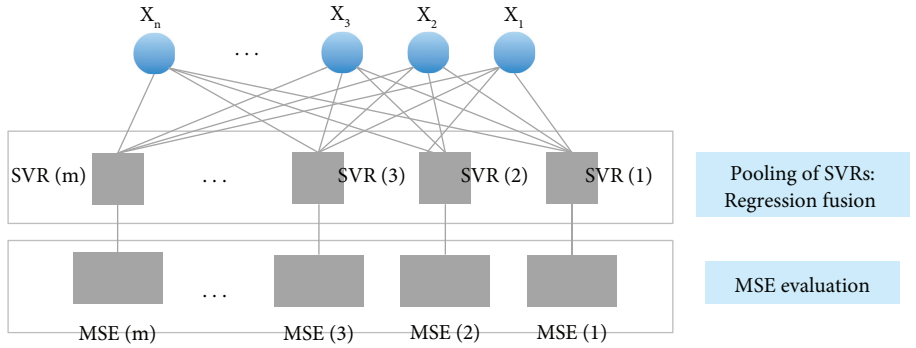

Figure 5: Regression fusion based on pooling the SVRs models.

Table 1: Practical data collected from the concrete laboratory of Imam Khomeini University of Sabzevar.

Data	Components	Max	Min	Average	Standard deviation	Variance ($\times 10^{-3}$)
Input (Kg in M^3)	Cement	383	142	240.40	79.02	6.24
	Water	199	0	73.14	60.52	3.66
	Fly ash	287	3.5	152.47	85.55	7.32
	Fine aggregate	244.35	176	200.83	20.35	0.423
	Coarse aggregate	25	3.12	12.92	3.73	0.134
	Superplasticizers	1118	631	887.13	88.37	7.839
	Slag	943	543.12	744.08	63.98	4.12
Output	FLOW (cm)	34.87	0	22.43	9.124	0.0831
	SLUMP (cm)	96	21	54.514	17.82	0.317
	28-day compressive (Mpa)	66.34	18.56	40.82	8.233	0.678

Table 2: Calculation of MSE, MAPE average, minimum, and maximum error for predicting high-strength lightweight concrete by the proposed regression fusion based on pool of SVRs and modified AIG algorithm. In this table, the K value in K-fold CV is considered to be equal to 5.

K-fold	Minimum error			Maximum error			MSE			MAPE		
	Output 1	Output 2	Output 3	Output 1	Output 2	Output 3	Output 1	Output 2	Output 3	Output 1	Output 2	Output 3
5-Fold (1)	0.273	0.383	0.317	14.31	21.18	9.53	1.73	4.59	1.24	0.965	1.53	0.894
5-Fold (2)	0.206	0.412	0.237	12.73	14.31	13.12	1.39	5.03	1.08	0.524	0.823	0.776
5-Fold (3)	0.229	0.374	0.365	10.33	28.73	14.43	1.58	4.87	1.44	0.947	1.34	0.739
5-Fold (4)	0.441	0.480	0.594	16.43	19.17	11.29	2.65	6.27	1.57	0.731	1.13	0.947
5-Fold (5)	0.202	0.711	0.254	15.45	29.83	16.56	2.61	9.07	0.794	0.575	0.767	0.722
5-Fold (6)	0.503	0.308	0.408	15.32	11.43	0.08	1.14	8.24	0.647	0.995	1.42	18.1
5-Fold (7)	0.153	0.494	0.211	17.40	15.87	9.86	1.09	9.01	0.733	0.673	0.865	0.712
5-Fold (8)	0.328	0.487	0.264	17.73	28.65	7.22	1.76	7.11	0.851	0.801	0.915	0.834
5-Fold (9)	0.162	0.374	0.183	16.56	26.73	13.25	2.11	8.14	0.578	0.787	1.27	0.912
5-Fold (10)	0.258	0.448	0.379	16.30	34.19	9.45	1.39	8.76	0.476	0.413	0.873	0.748
Avg.		0.347			16.248			3.262			1.4576	

outputs, including cement, slag, fly ash, water, superplasticizers, coarse aggregate, and fine aggregate. All of these inputs are in component kg in one M^3 concrete. Besides, the outputs of this dataset are SLUMP (cm), FLOW (cm), and 28-day Compressive Strength (Mpa). The number of constructed specimens is higher than the first data samples (243 specimens), and the number of feature inputs and outputs is equal. The necessary information of this dataset is shown in Table 1.

4.2. Assessments. As presented in Table 2, regression predictions for datasets are a combination of different algorithms at the time of testing by selection K value equal to 5. Changing the values of RBF parameters and preventing overfitting in many repetitions, the SVRs pool as regression fusion was used to find the lowest amount of MSE among the five structures in each pool.

If the MSE is less than 5% of the total error in the sample data in this structure, the corresponding SVR is selected as the base network. Otherwise, the minimum MSE and the corresponding network structure should be chosen. Figure 6 shows the results of the RMSE convergence and corresponding Loss function of the algorithm set to reach the minimum value. When the algorithm tries to achieve the optimal value in the training step, more satisfactory outputs

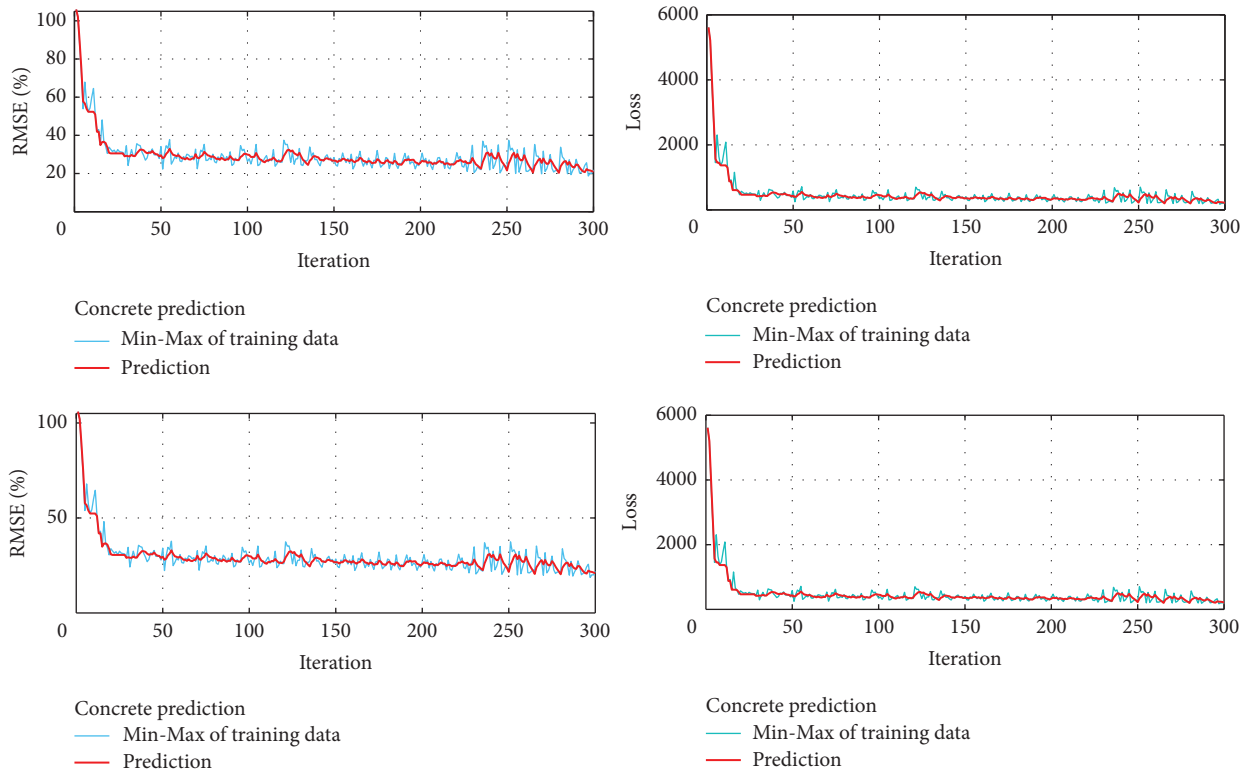

Figure 6: RMSE convergence and corresponding Loss function in training step.

Table 3: Calculation of MSE, MAPE average, minimum, and maximum error for predicting high-strength lightweight concrete by the proposed regression fusion based on pool of SVRs and modified AIG algorithm. In this table, the K value in K-fold CV is considered to be equal to 10.

K-fold	Minimum error			Maximum error			MSE			MAPE		
	Output 1	Output 2	Output 3	Output 1	Output 2	Output 3	Output 1	Output 2	Output 3	Output 1	Output 2	Output 3
10-Fold (1)	0.254	0.418	0.339	13.74	20.23	10.65	1.80	4.53	1.28	0.932	1.41	0.844
10-Fold (2)	0.211	0.467	0.166	11.53	13.56	7.83	1.64	5.17	1.12	0.556	0.794	0.760
10-Fold (3)	0.287	0.456	0.373	11.76	27.31	5.22	1.48	4.75	0.98	0.971	1.11	0.734
10-Fold (4)	0.411	0.434	0.622	16.05	17.37	10.09	2.23	6.31	1.01	0.754	1.32	0.978
10-Fold (5)	0.228	0.773	0.267	14.37	24.13	5.76	2.42	8.94	0.765	0.543	0.732	0.651
10-Fold (6)	0.537	0.491	0.418	16.29	19.29	8.53	1.06	8.07	0.678	0.986	1.20	1.12
10-Fold (7)	0.243	0.565	0.467	15.81	13.91	11.51	1.12	9.12	0.743	0.640	0.876	0.793
10-Fold (8)	0.375	0.437	0.241	16.29	26.44	8.97	1.43	6.88	0.876	0.813	0.967	0.867
10-Fold (9)	0.291	0.414	0.212	18.16	29.23	6.13	2.08	7.95	0.561	0.804	1.13	0.946
10-Fold (10)	0.243	0.473	0.356	15.27	30.89	7.38	1.51	8.37	0.441	0.587	0.663	0.331
Avg.	0.382	12.387	3.148	0.8637								

can be obtained in the experimental section by increasing the number of search alterations of the AIG algorithm or increasing the number of SVRs.

The change in evaluation criteria is not significant due to the change in K, and thus, Table 3 shows that a slight improvement in K accompanies the experiment.

However, although the training phase results are done offline, due to the numerous repetitions in finding the best SVR structure of the learning pool and the time-consuming AIG optimization algorithm, computational complexity is observed, especially in the training step. A similar implementation for random data in convergence to the optimal value for four validation data is shown in Figure 7. In these plots, a limited number of repetitions are seen, and the level of error originates from the training stage.

On average, for each run of the algorithm, the average value of correlation is greater than 0.9 and, in some cases, reaches as high as 0.98. Assuming that, in the prediction of concrete quality regression, y_t and x_t are static variables in the detection or estimation of parameters and T and F tests, the results were used by increasing the sample size, and sample variance to population variance was used to

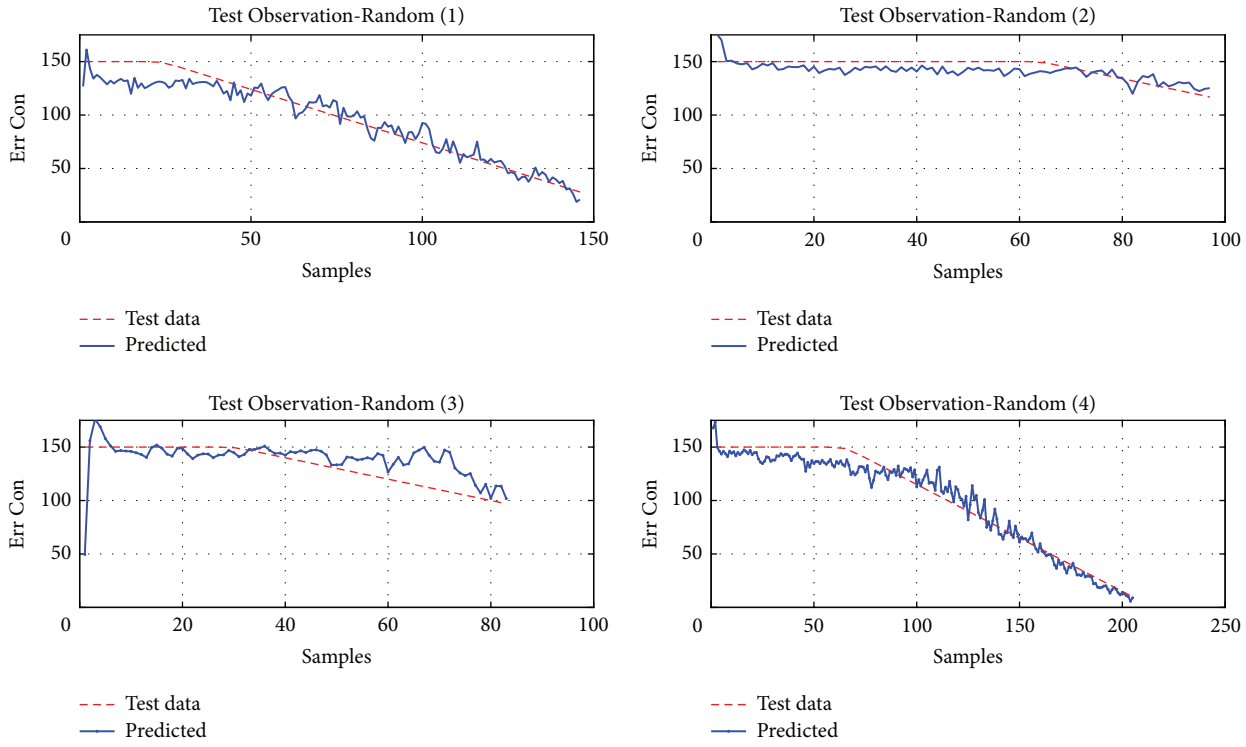

Figure 7: Algorithm convergence to minimum error for four random validation data with limited number of iterations.

demonstrate minimal normal consistency. Estimating the MES for an estimate of the predicted time sequence with dynamic properties may suggest that the variance has not been well defined. Therefore, this value will not fluctuate around a specific mean. To further explain the variables y_t and x_t, it was assumed that the regression trend was defined as the quality prediction trend in a random step:

$$\begin{aligned} y_t &= y_{t-1} + \varepsilon_1 t \quad (t = 1, \ldots, N), \\ x_t &= x_{t-1} + \varepsilon_2 t \quad (t = 1, \ldots, N), \end{aligned} \tag{17}$$

where $\varepsilon_1 t$ and $\varepsilon_2 t$ had independent distribution functions, and the relationship between the variables y_t and x_t was not justifiable.

To perform a regression analysis, we first assumed a relationship between the two variables selected from the seven input variables. Based on the assumption that there is a linear relationship between the two variables, quantitative data was collected from both variables, and the data were plotted as points on a two-dimensional map. As shown in Figure 8, the difference between the main and predicted outputs is small, and the variances between them are negligible. Table 4 shows the calculated variances of ten experiments. Variances indicate great independence of the features selected by SPSS software. Therefore, using the output quality, a small portion of the low-impact features can be distinguished from the others.

As noted earlier, concrete strength is defined in terms of its ingredients, weight, and specific properties. Data were obtained under laboratory conditions based on real conditions. Other factors such as data collection, mixing, and other parameters affecting concrete strength are also included in this section. Although the laboratory data presented in some studies offer valuable information on this subject, there were essential details, the absence of which could significantly predict performance in many cases.

5. Discussion

In concrete preparation by learning-based methods, the most crucial design issue is the lack of significant differences between the predicted outputs and the actual output. Hence, the R-Squared is considered as one of the most specific criteria for comparison between methods, where y, $\hat{y}$, and $\overline{y}$ are the main, mean, and predicted values, respectively. The R-Squared is expressed as (19):

$$R^2(y, \hat{y}) = 1 - \frac{\sum_{i=1}^{n} (y_i - \hat{y})^2}{\sum_{i=1}^{n} (y_i - \overline{y})^2}. \tag{18}$$

In these experiments, different test conditions are investigated:

(1) When SVR is used alone in estimating outputs (Model 1).

(2) When fusion between SVRs is used in estimation (Model 2).

(3) When the fusion between SVRs is combined with the genetic algorithm in the analysis (Model 3).

(4) When the fusion between SVRs is combined with the PSO algorithm in the estimation (Model 4).

(5) When the fusion between SVRs is combined with the AIG algorithm in the estimate (Model 5).

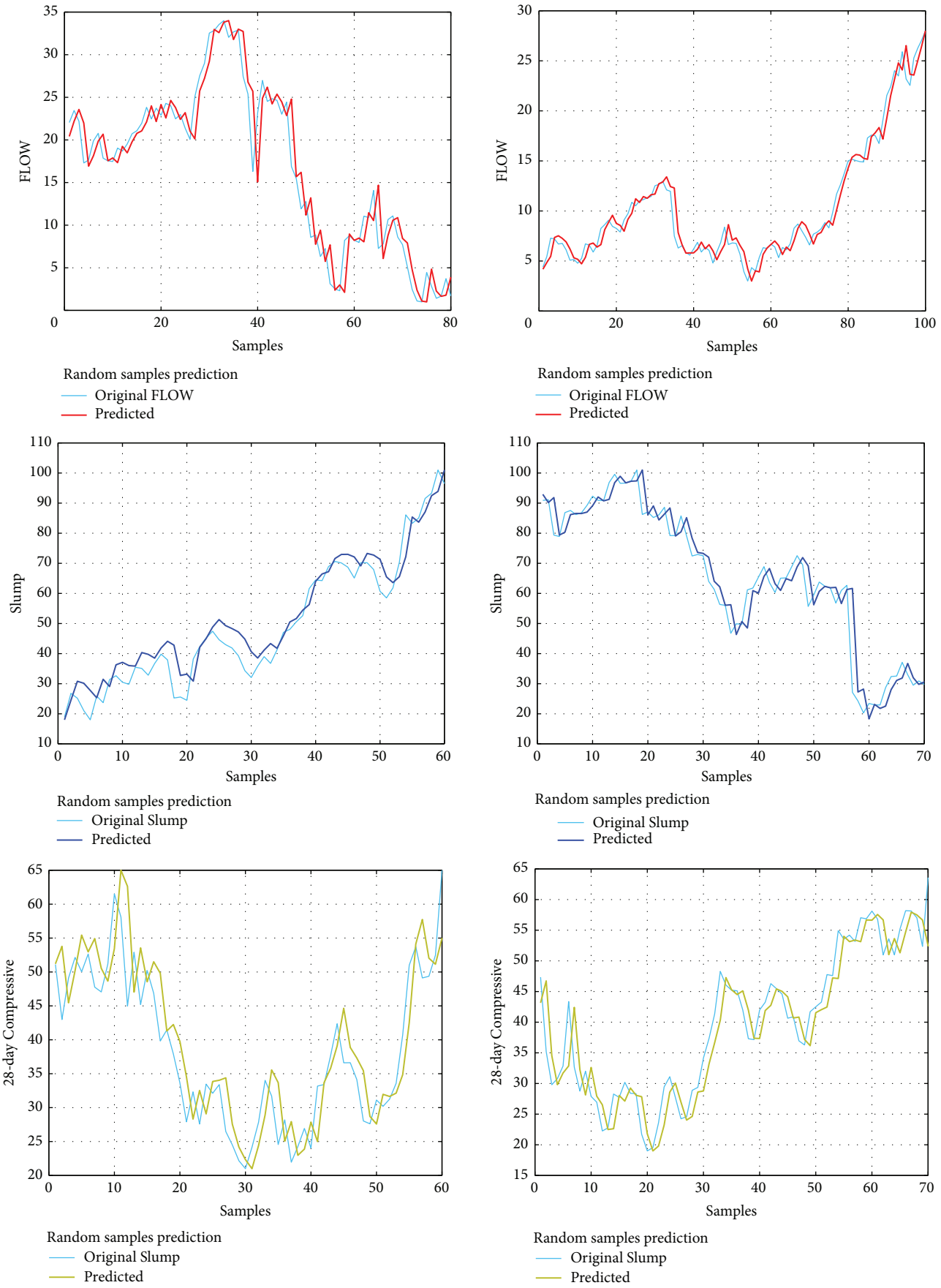

Figure 8: Difference between the main and predicted outputs of test step is small, and the variances between them are negligible.

Table 4: Computed variances in 10 experiments: blue arrows indicate that the final variance between the main outputs and the forecast is small compared to experts' opinions. Red arrows also denote higher variance compared to experts' opinions.

Experiments	Expert 1	Expert 2	Simple SVR	Fusion-SVRs (linear)	Fusion- SVRs (RBF)	Fusion- SVRs (RBF)-AIG	Fusion-SVRs-(RBF)-mAIG
1	±1.18	±1.67	±3.03	±2.27	±2.04	±1.29	±0.96 ↑
2	±1.43	±1.28	±4.17	±3.83	±2.46	±1.13	±0.85 ↑
3	±1.83	±1.65	±4.22	±3.47	±2.72	±2.57	±1.39 ↑
4	±2.11	±1.68	±5.84	±3.13	±2.51	±1.21	±0.75 ↑
5	±1.78	±2.07	±5.12	±4.73	±3.62	±3.16	±2.11 ↓
6	±1.91	±1.69	±3.19	±2.48	±2.92	±1.94	±1.06 ↑
7	±1.44	±1.73	±4.41	±2.36	±2.08	±1.37	±0.84 ↑
8	±2.33	±2.27	±5.93	±4.27	±3.63	±2.71	±1.48 ↑
9	±1.76	±2.44	±5.51	±3.26	±2.71	±1.28	±1.02 ↑
10	±1.45	±1.61	±4.31	±3.44	±2.59	±2.42	±1.76 ↓

(6) When the fusion between SVRs is combined with the modified AIG algorithm in the estimation (Model 6).

Experimental representations for five different and random types of data are shown in Figure 9 separately for each of the six models. The p-value in the proposed algorithm indicated a significant relationship between the proposed algorithm's output and regression values. For this reason, we rounded the outputs ($p < 0.05$), which manifest the significance of outputs. The comparison with other similar outputs and methods provides a valid justification for rejecting the null hypothesis (H_0). This is because the test result was not in the acceptable range of H_0 and thus H_0 was not confirmed ($\alpha = 0.05$) and therefore $-Z_{\alpha-1}$ is equal to -1.65. This meant that the confidence interval was greater than 95% and the outputs more accurately resembled reality, as indicated by the studied samples and K-equal validation. To test the claims regarding the correlation of concrete properties, aside from selection by the genetic algorithms, SPSS software was used to analyze the correlation factor between the measured properties. The results were significantly identical and except for the fifth feature (which had a lower correlation compared to other coefficients), features with 100% correlation were selected correctly.

However, as noted in Abrams' law, in real weather conditions, other factors may also affect the mixture of substances. This rule, which predicts concrete performance based on a combination of water-cement mixture, indicated a slight error for the coefficient of determination. This could be attributed to water interference in the hydration process of cement, which can cause changes in the molecular structure of cement material and thus affect the process of achieving optimal concrete performance.

We know that concreting at a temperature of less than 5 °C slows down the hydration process, and the process of obtaining concrete strength practically stops. As the temperature of concrete decreases, its hardening and achieving strength decreases, and at the temperature below freezing point, the chemical process of hardening of concrete stops. In general, at low temperatures, the rate of gain of concrete strength decreases. Experiments were performed after producing the concrete, which was considered for the built concretes according to the regional conditions and the occurrence of frost.

In the experiments, the decrease of temperature and change of each of the outputs is considered noise, and the algorithm's resistance to change of each of the concrete components is investigated. The effect of freezing is measured, and the temperature drop is considered as the fourth output. It was found that, among the primary materials, changes in some of them can significantly prevent concrete from freezing. In general, for a given degree of hydration, the higher the water-to-cement ratio, or for an offered water-to-cement rate, the lower the degree of hydration, and the larger the pore volume in the hydrated cement paste. Since freezing water settles quickly in large pores, it can be hypothesized that the amount of freezing water for water-to-cement ratios is higher and, in the early processing times at a given freezing temperature, will be more. By performing the above software tests on typical weight concretes exposed to freezing and thawing in wet conditions, the maximum water-to-cement ratio should be considered for tabulations, water ducts, and guardrails, or parts thereof equal to 0.45 and equal to 0.5 for the remaining pieces. It is clear that these water limits to cement ratio are based on the assumption of sufficient hydration of cement. In other words, the amount of water that can freeze in concrete with a specific rate of water to cement increases with decreasing temperature, and the amount of water that freezes at a particular temperature increases with an increasing ratio of water to cement. Based on this, it was concluded that as the temperature decreases, the water-to-cement rate should be considered, and the combination of some slags should be used more sensitively.

High error, computational complexity, and uncertainty challenges in algorithms are common problems in quality recognition optimization methods. Table 5 presents the analytical comparison between the former techniques and the proposed approach. They also tried to predict the compressive strength of lightweight structural concrete.

Future designs should incorporate deep learning models that are transferable, such as transfer learning structures [55, 56]. Optimization algorithms as well as deep learning based on neural networks have a major impact on the classification process. Except for the optimization method

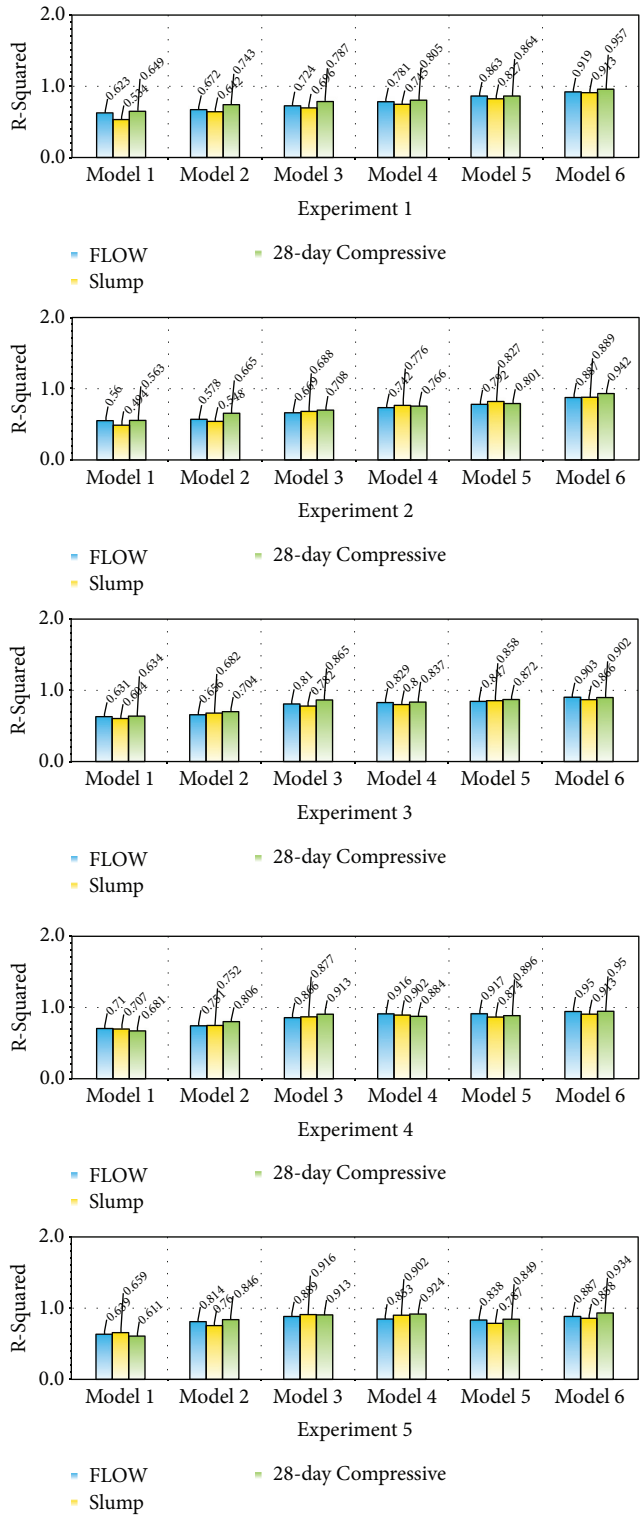

Figure 9: R-Squared estimation in six different models for all three outputs in concrete production and display of experiments for 5 random types of data.

employed in the paper, some of the most representative computational intelligence algorithms can be utilized to solve the challenges of high-quality concrete prediction. Some recent optimization algorithms include monarch butterfly optimization (MBO) [57], earthworm optimization algorithm (EWA) [58], elephant herding optimization (EHO) [59], moth search (MS) algorithm [60], Slime mould algorithm (SMA) [61], and Harris hawks optimization (HHO) [62].

Table 5: Comparison of the proposed algorithm to similar approaches based on used assessments.

Method	Optimization technique	Learning model	Dataset	Results
Atici [11]	-	Multivariate regression analysis and artificial neural network	Collected data	Optimal accuracy in regression analysis (90%)
Rahchamani et al. [14]	GBMO	ANFIS regression learner	UCI and collected data	MSEs for testing step were 1.065 to 3.16 respectively
Sadowski et al. [21]	CCA	Neural networks regression analysis	Collected data	MSE in the training and testing were 0.157 and 0.024 respectively
Zarandi et al [22]	-	Fuzzy neural network regression analysis	Collected data	Correlation factor in training and testing steps was 90% and 96% respectively
Chandwani et al. [26]	GA	Regression analysis of neural network	Collected data	MAPE for training and testing was 4% to 19% respectively
Nikoo et al. [27]	GA	Multilayer neural networks regression analysis	Collected data	MSE for training and testing was 0.09 to 0.813 respectively
Sadowski et al. [47]	PCA and GA	Neural Networks/Self-Organizing maps (SOM)	Collected data	MSE in the training and testing were 0.006 and 0.007 respectively
Behnood et al. [48]	Multi-objective grey wolves	Neural networks regression analysis	Collected data	Correlation coefficient is 0.96
Yaman et al [49]	-	Self-compacting concrete using artificial neural network	Collected data	R^2 is 0.65 to 1
Alshihri et al. [50]	-	Neural network regression analysis	Collected data	MAE for training and testing was 1% and 3% respectively.
Tsai et al. [51]	PSO	Cascaded neural network regression analysis	Collected data	Index values were not computed
Madandoust et al. [52]	GA	Regression analysis of neural network	Collected data	Maximum error in the training and testing was 9% to 13% respectively
Yeh et al. [53]	-	Second-order neural network regression analysis	UCI database [54] (103 samples)	RMSE for training and testing was 5% to 10% respectively
Proposed	Modified AIG	Regression fusion based on pool of SVRs	Collected data	MSEs for testing step were 0.7 to 3.2

6. Conclusion

Predicting the quality of high-strength concrete is a critical issue in the concrete industry. Our investigations in this paper showed that using an improved model, including the fusion of multiple SVR networks and the modified AIG algorithm, can produce satisfactory outcomes in predicting 28-day compressive strength. Unlike previous methods, which only work in fabricating concrete compositions, the estimator model utilizes a fast yet efficient model and facilitates the regression classification process. The research results suggest that the degree of complexity in the sample data can be reduced to establish a correlation in a standard pattern between the features. Accordingly, it can be concluded that employing the proposed method as an automated method can facilitate the analysis of concrete data and, therefore, offers an accurate estimation of the quality of high-strength concrete. In the future, the authors will use several statistical criteria and various machine learning models for further and more extensive investigation. Furthermore, the use of fusion between neural networks (considering the challenge of uncertainty) and support vectors can be effective in mapping input data and extracting the appropriate pattern.

Data Availability

All the data and codes are available from the corresponding authors.

Ethical Approval

The research meets all applicable standards with regard to the ethics of experimentation and research integrity, and the following is being certified/declared true. As an expert scientist and along with co-authors of concerned field, the paper has been submitted with full responsibility, following due ethical procedure, and there is no duplicate publication, fraud, plagiarism, or concerns about animal or human experimentation.

Conflicts of Interest

The authors have no conflicts of interest to declare.

Authors' Contributions

Gh. Rahchamani and S. M. Movahedifar conceived and planned the experiments. A. Honarbakhsh and Gh. Rahchamani planned and carried out the simulations. A. Honarbakhsh and Gh. Rahchamani contributed to the interpretation of the results. Gh. Rahchamani, S. M. Movahedifar, and A. Honarbakhsh took the lead in writing the manuscript. All authors provided critical feedback and helped shape the research, analysis, and manuscript.

Acknowledgments

The authors gratefully acknowledge the generous support of Imam Khomeini University of Sabzevar and Islamic Azad University of Neyshabur. The authors wish to thank experts from the New Materials Technology and Processing Research Center of Neyshabur for the realization of this project.

References

[1] K. Samrajyam, B. Sobha, T. G. Rao, and R. S. Prasad, "Plastic optic fiber (POF) based phase difference measurement method for estimation of crack mouth opening displacement (CMOD) in concrete," *i-manager's Journal on Civil Engineering*, vol. 4, no. 2, pp. 2231–1068, 2014.

[2] N. Makul, "Modern sustainable cement and concrete composites: review of current status, challenges and guidelines," *Sustainable Materials and Technologies*, vol. 25, Article ID e00155, 2020.

[3] Z. Leng, Z. Tan, H. Yu, and J. Guo, "Improvement of storage stability of SBS-modified asphalt with nanoclay using a new mixing method," *Road Materials and Pavement Design*, vol. 20, no. 7, pp. 1601–1614, 2019.

[4] J. Opon and M. Henry, "An indicator framework for quantifying the sustainability of concrete materials from the perspectives of global sustainable development," *Journal of Cleaner Production*, vol. 218, pp. 718–737, 2019.

[5] M. K. Haridharan, S. Matheswaran, G. Murali et al., "Impact response of two-layered grouted aggregate fibrous concrete composite under falling mass impact," *Construction and Building Materials*, vol. 263, Article ID 120628, 2020.

[6] D. Darwin, C. W. Dolan, and A. H. Nilson, *Design of concrete Structures*, McGraw-Hill Education, New York, 2016.

[7] D. Sobhani, S. Zarei, H. Savoj, and M. Shayanfar, "Investigation on corrosion effects of reinforcement on the moment-curvature diagram of reinforced concrete sections," *Mapta Journal of Architecture, Urbanism and Civil Engineering (MJAUCE)*, vol. 1, no. 3, pp. 11–22, 2018.

[8] C. Zhou, Y. Feng, and Z. Yin, "Maintaining complex formations and avoiding obstacles for multi-agents," *Computers, Materials & Continua*, vol. 62, no. 2, pp. 877–891, 2020.

[9] S. Lee, Y. Ahn, and H. Young Kim, "Predicting concrete compressive strength using deep convolutional neural network based on image characteristics," *Computers, Materials & Continua*, vol. 65, no. 1, pp. 1–17, 2020.

[10] P. G. Asteris and V. G. Mokos, "Concrete compressive strength using artificial neural networks," *Neural Computing & Applications*, vol. 32, no. 15, pp. 11807–11826, 2020.

[11] U. Atici, "Prediction of the strength of mineral admixture concrete using multivariable regression analysis and an artificial neural network," *Expert Systems with Applications*, vol. 38, no. 8, pp. 9609–9618, 2011.

[12] D. Dao, H.-B. Ly, S. Trinh, T.-T. Le, and B. Pham, "Artificial intelligence approaches for prediction of compressive strength of geopolymer concrete," *Materials*, vol. 12, no. 6, p. 983, 2019.

[13] A. Shiuly, N. Roy, and R. B. Sahu, "Prediction of peak ground acceleration for Himalayan region using artificial neural network and genetic algorithm," *Arabian Journal of Geosciences*, vol. 13, no. 5, pp. 1–10, 2020.

[14] G. Rahchamani, S. M. Movahedifar, and A. Honarbakhsh, "A hybrid optimized learning-based compressive performance of concrete prediction using GBMO-ANFIS classifier and genetic algorithm reduction," *Structural Concrete*, vol. 22, p. E779, 2021.

[15] N. D. Hoang, Q. L. Nguyen, and X. L. Tran, "Automatic detection of concrete spalling using piecewise linear stochastic gradient descent logistic regression and image texture analysis," *Complexity*, vol. 2019, Article ID 5910625, 14 pages, 2019.

[16] V. Chandwani, V. Agrawal, and R. Nagar, "Modeling slump of ready mix concrete using genetically evolved artificial neural networks," *Advances in Artificial Neural Systems*, vol. 2014, Article ID 629137, 9 pages, 2014.

[17] J. A. Bogas, M. G. Gomes, and A. Gomes, "Compressive strength evaluation of structural lightweight concrete by non-destructive ultrasonic pulse velocity method," *Ultrasonics*, vol. 53, no. 5, pp. 962–972, 2013.

[18] T. T. Nguyen, H. Pham Duy, T. Pham Thanh, and H. H. Vu, "Compressive strength evaluation of fiber-reinforced high-strength self-compacting concrete with artificial intelligence," *Advances in Civil Engineering*, vol. 2020, Article ID 3012139, 12 pages, 2020.

[19] J.-S. Chou, C.-K. Chiu, M. Farfoura, and I. Al-Taharwa, "Optimizing the prediction accuracy of concrete compressive strength based on a comparison of data-mining techniques," *Journal of Computing in Civil Engineering*, vol. 25, no. 3, pp. 242–253, 2011.

[20] Q. B. Pham, H. A. Afan, B. Mohammadi et al., "Hybrid model to improve the river streamflow forecasting utilizing multi-layer perceptron-based intelligent water drop optimization algorithm," *Soft Computing*, vol. 24, pp. 18039–18056, 2020.

[21] L. Sadowski and M. Nikoo, "Corrosion current density prediction in reinforced concrete by imperialist competitive algorithm," *Neural Computing & Applications*, vol. 25, no. 7-8, pp. 1627–1638, 2014.

[22] M. F. Zarandi, I. B. Türksen, J. Sobhani, and A. A. Ramezanianpour, "Fuzzy polynomial neural networks for approximation of the compressive strength of concrete," *Applied Soft Computing*, vol. 8, no. 1, pp. 488–498, 2008.

[23] M. Nikoo, P. Zarfam, and H. Sayahpour, "Determination of compressive strength of concrete using self organization feature map (SOFM)," *Engineering with Computers*, vol. 31, no. 1, pp. 113–121, 2015.

[24] A. Johari, A. A. Javadi, and G. Habibagahi, "Modelling the mechanical behaviour of unsaturated soils using a genetic algorithm-based neural network," *Computers and Geotechnics*, vol. 38, no. 1, pp. 2–13, 2011.

[25] A. R. Ghanizadeh, H. Abbaslou, A. T. Amlashi, and P. Alidoust, "Modeling of bentonite/sepiolite plastic concrete compressive strength using artificial neural network and support vector machine," *Frontiers of Structural and Civil Engineering*, vol. 13, no. 1, pp. 215–239, 2019.

[26] V. Chandwani, V. Agrawal, and R. Nagar, "Modeling slump of ready mix concrete using genetic algorithms assisted training of Artificial Neural Networks," *Expert Systems with Applications*, vol. 42, no. 2, pp. 885–893, 2015.

[27] M. Nikoo, F. Torabian Moghadam, and Ł. Sadowski, "Prediction of concrete compressive strength by evolutionary artificial neural networks," *Advances in Materials Science and Engineering*, vol. 2015, Article ID 849126, 8 pages, 2015.

[28] M. Shariati, M. S. Mafipour, P. Mehrabi et al., "Application of a hybrid artificial neural network-particle swarm optimization (ANN-PSO) model in behavior prediction of channel shear connectors embedded in normal and high-strength concrete," *Applied Sciences*, vol. 9, no. 24, p. 5534, 2019.

[29] M. Ayubi Rad and M. S. Ayubirad, "Comparison of artificial neural network and coupled simulated annealing based least square support vector regression models for prediction of compressive strength of high-performance concrete," *Scientia Iranica*, vol. 24, no. 2, pp. 487–496, 2017.

[30] T. A. Nguyen, H. B. Ly, H. V. T. Mai, and V. Q. Tran, "Prediction of later-age concrete compressive strength using feedforward neural network," *Advances in Materials Science and Engineering*, vol. 2020, Article ID 9682740, 8 pages, 2020.

[31] T. Nguyen, A. Kashani, T. Ngo, and S. Bordas, "Deep neural network with high-order neuron for the prediction of foamed concrete strength," *Computer-Aided Civil and Infrastructure Engineering*, vol. 34, no. 4, pp. 316–332, 2019.

[32] J. Guo, M. Li, L. Wang et al., "Estimating cement compressive strength using three-dimensional microstructure images and deep belief network," *Engineering Applications of Artificial Intelligence*, vol. 88, Article ID 103378, 2020.

[33] Y. Jang, Y. Ahn, and H. Y. Kim, "Estimating compressive strength of concrete using deep convolutional neural networks with digital microscope images," *Journal of Computing in Civil Engineering*, vol. 33, no. 3, Article ID 04019018, 2019.

[34] E. Sadrossadat and H. Basarir, "An evolutionary-based prediction model of the 28-day compressive strength of high-performance concrete containing cementitious materials," *Advances in Civil Engineering Materials*, vol. 8, no. 3, pp. 484–497, 2019.

[35] M. Lieder, F. M. Asif, A. Rashid, A. Mihelič, and S. Kotnik, "Towards circular economy implementation in manufacturing systems using a multi-method simulation approach to link design and business strategy," *International Journal of Advanced Manufacturing Technology*, vol. 93, no. 5, pp. 1953–1970, 2017.

[36] Y. Yu, W. Li, J. Li, and T. N. Nguyen, "A novel optimised self-learning method for compressive strength prediction of high performance concrete," *Construction and Building Materials*, vol. 184, pp. 229–247, 2018.

[37] Y. Yu, T. N. Nguyen, J. Li, L. F. Sanchez, and A. Nguyen, "Predicting elastic modulus degradation of alkali silica reaction affected concrete using soft computing techniques: a comparative study," *Construction and Building Materials*, vol. 274, Article ID 122024, 2021.

[38] Y. Yu, C. Zhang, X. Gu, and Y. Cui, "Expansion prediction of alkali aggregate reactivity-affected concrete structures using a hybrid soft computing method," *Neural Computing & Applications*, vol. 31, no. 12, pp. 8641–8660, 2019.

[39] K. Shaswat, "Concrete slump prediction modeling with a fine-tuned convolutional neural network: hybridizing sea lion and dragonfly algorithms," *Environmental Science and Pollution Research*, vol. 2021, pp. 1–12, 2021.

[40] T. N. Nguyen, Y. Yu, J. Li, N. Gowripalan, and V. Sirivivatnanon, "Elastic modulus of ASR-affected concrete: an evaluation using artificial neural network," *Computers and Concrete*, vol. 24, 2019.

[41] P. Pijarski and P. Kacejko, "A new metaheuristic optimization method: the algorithm of the innovative gunner (AIG)," *Engineering Optimization*, vol. 51, pp. 2049–2068, 2019.

[42] C. Cortes and V. Vapnik, "Support-vector networks," *Machine Learning*, vol. 20, no. 3, pp. 273–297, 1995.

[43] K. Rezaee and S. Zolfaghari, "A Direct Classification Approach to Recognize Stress Levels in Virtual Reality Therapy for Patients with Multiple Sclerosis," *Computational Intelligence*, vol. 38, 2021.

[44] N. Tavasoli, K. Rezaee, M. Momenzadeh, and M. Sehhati, "An ensemble soft weighted gene selection-based approach and cancer classification using modified metaheuristic learning," *Journal of Computational Design and Engineering*, vol. 8, no. 4, pp. 1172–1189, 2021.

[45] R. Li, Y. Liu, Y. Qiao, T. Ma, B. Wang, and X. Luo, "Street-level landmarks acquisition based on SVM classifiers," *CMC-Computers Materlals & Continua*, vol. 59, no. 2, pp. 591–606, 2019.

[46] K. Rezaee, J. Haddadnia, and M. Rasegh Ghezelbash, "A novel algorithm for accurate diagnosis of hepatitis B and its severity," *International Journal of Hospital Research*, vol. 3, no. 1, pp. 1–10, 2014.

[47] Ł. Sadowski, M. Nikoo, and M. Nikoo, "Principal component analysis combined with a self organization feature map to determine the pull-off adhesion between concrete layers," *Construction and Building Materials*, vol. 78, pp. 386–396, 2015.

[48] A. Behnood and E. M. Golafshani, "Predicting the compressive strength of silica fume concrete using hybrid artificial neural network with multi-objective grey wolves," *Journal of Cleaner Production*, vol. 202, pp. 54–64, 2018.

[49] M. A. Yaman, M. Abd Elaty, and M. Taman, "Predicting the ingredients of self compacting concrete using artificial neural network," *Alexandria Engineering Journal*, vol. 56, no. 4, pp. 523–532, 2017.

[50] M. M. Alshihri, A. M. Azmy, and M. S. El-Bisy, "Neural networks for predicting compressive strength of structural light weight concrete," *Construction and Building Materials*, vol. 23, no. 6, pp. 2214–2219, 2009.

[51] H. C. Tsai, "Predicting strengths of concrete-type specimens using hybrid multilayer perceptrons with center-unified particle swarm optimization," *Expert Systems with Applications*, vol. 37, no. 2, pp. 1104–1112, 2010.

[52] R. Madandoust, R. Ghavidel, and N. Nariman-Zadeh, "Evolutionary design of generalized GMDH-type neural network for prediction of concrete compressive strength using UPV," *Computational Materials Science*, vol. 49, no. 3, pp. 556–567, 2010.

[53] I. Yeh, "Modeling slump of concrete with fly ash and superplasticizer," *Computers and Concrete*, vol. 5, no. 6, pp. 559–572, 2008.

[54] I. C. Yeh, "Exploring concrete slump model using artificial neural networks," *Journal of Computing in Civil Engineering*, vol. 20, no. 3, pp. 217–221, 2006.

[55] K. Rezaee, S. Savarkar, X. Yu, and J. Zhang, "A hybrid deep transfer learning-based approach for Parkinson's disease classification in surface electromyography signals," *Biomedical Signal Processing and Control*, vol. 71, Article ID 103161, 2022.

[56] K. Rezaee, S. M. Rezakhani, M. R. Khosravi, and M. K. Moghimi, "A survey on deep learning-based real-time crowd anomaly detection for secure distributed video surveillance," *Personal and Ubiquitous Computing*, vol. 2021, pp. 1–17, 2021.

[57] G. G. Wang, S. Deb, and Z. Cui, "Monarch butterfly optimization," *Neural Computing and Applications*, vol. 31, no. 7, pp. 1995–2014, 2019.

[58] G. G. Wang, S. Deb, and L. D. S. Coelho, "Earthworm optimisation algorithm: a bio-inspired metaheuristic algorithm for global optimisation problems," *International Journal of Bio-Inspired Computation*, vol. 12, no. 1, pp. 1–22, 2018.

[59] G. G. Wang, S. Deb, and L. D. S. Coelho, "Elephant herding optimization," in *Proceedings of the 2015 3rd International Symposium on Computational and Business Intelligence (ISCBI)*, pp. 1–5, IEEE, Bali, Indonesia, 2015, December.

[60] G. G. Wang, "Moth search algorithm: a bio-inspired metaheuristic algorithm for global optimization problems," *Memetic Computing*, vol. 10, no. 2, pp. 151–164, 2018.

[61] S. Li, H. Chen, M. Wang, A. A. Heidari, and S. Mirjalili, "Slime mould algorithm: a new method for stochastic optimization," *Future Generation Computer Systems*, vol. 111, pp. 300–323, 2020.

[62] A. A. Heidari, S. Mirjalili, H. Faris, I. Aljarah, M. Mafarja, and H. Chen, "Harris hawks optimization: algorithm and applications," *Future Generation Computer Systems*, vol. 97, pp. 849–872, 2019.